28th AIAA Applied Aerodynamics Conference
28 June - 1 July 2010, Chicago, Illinois

AIAA 2010-4679

Investigation of Utilizing a Single Surface Depression in the Optimisation of NLF Aerofoil Design

R. McRoberts[1], J.M. Early[2], S. Spence[3]

School of Mechanical and Aerospace Engineering,
Queen's University, Belfast, BT9 5AG, Northern Ireland

& H. Medina[4]

School of Mechanical and Automotive Engineering,
Coventry University, Coventry, CV1 5FB, United Kingdom

An environment has been created for the optimisation of aerofoil profiles with inclusion of small surface features. For TS wave dominated flows, the paper examines the consequences of the addition of a depression on the aerodynamic optimisation of an NLF aerofoil, and describes the geometry definition fidelity and optimisation algorithm employed in the development process. The variables that define the depression for this optimisation investigation have been fixed, however a preliminary study is presented demonstrating the sensitivity of the flow to the depression characteristics. Solutions to the optimisation problem are then presented using both gradient-based and genetic algorithm techniques, and for accurate representation of the inclusion of small surface perturbations it is concluded that a global optimisation method is required for this type of aerofoil optimisation task due to the nature of the response surface generated. When dealing with surface features, changes in the transition onset are likely to be of a non-linear nature so it is highly critical to have an optimisation algorithm that is robust, suggesting that for this framework, gradient-based methods alone are not suited.

I. Introduction

Emerging ecological targets have placed the aviation industry under increasing pressure to significantly reduce harmful environmental emissions at all stages of the aircraft lifecycle. Many innovative techniques are being developed ranging from new materials and novel fuels, through to enhanced contouring of aerolines to improve performance. Complimentary to this, laminar flow control (LFC) methods have gained momentum in recent years, but the prediction of many of the features which affect transition and transition onset continues to be a challenge for the aerospace community (Atkin, 2008, Crouch, 1997, Reshotko, 1994, Joslin, 1998, Saric, 2004 give an overview of some of the more recent work in this area).

It has long been accepted that surface finish is critical to the achievement of extended laminar flow on aerodynamic surfaces (Gaster, 2005, Choi & Fujisawa, 1997) with protuberances that extend into laminar boundary layers subject to critical tolerances. Below this critical tolerance, the appreciable influence on the observable stability characteristic is thought to be negligible. When the effect of a depression is examined, it has been found that the effect on the transitional behavior due to the depression was much less prominent than for an equivalent protrusion (Baumann & Kind, 2001). The traditional perspective is that once the critical tolerance to affect the stability characteristics has been reached, the result is adverse, hastening the breakdown to turbulence. The actual influence of depression geometry is still not entirely clear - Nayfeh (1987) indicated that the dominating geometric parameters are the height-to-length ratio and the location of the imperfection, but there has been contradictory evidence as to the relative importance of the shape (Nayfeh, 1987, Holmes, 1992).

[1] Research Student, School of Mechanical and Aerospace Engineering, AIAA Student Member
[2] Lecturer, School of Mechanical and Aerospace Engineering, AIAA Senior Member
[3] Senior Lecturer, School of Mechanical and Aerospace Engineering
[4] Senior Lecturer, School of Mechanical and Automotive Engineering

Aerodynamic shape optimisation has become widely popular in the aerospace industry, as it enables large numbers of design variables relative to objective functions to be assessed to improve desirable attributes of aircraft performance. As the quality of the surface finish is clearly significant in attaining extensions of laminar flow, it is advantageous to include known imperfections in the design optimisation process to assist in the assessment of surface features, such as joints, on the aerodynamic characteristics as early as possible.

The computational cost of optimising features in many aerodynamic applications can be exceptionally large for the accessible resources; therefore methods that reduce the number of design variables for geometric features are of particular interest. This study assesses the viability of creating an optimisation framework for producing NLF aerofoils with the inclusion of surface features. An optimisation environment has been developed which uses a geometric representation technique to lessen the number of design variables defining an aerofoil profile, on which a surface feature is then superimposed. Boundary layer stability calculations are subsequently performed, and the transition onset location used as the objective function. For the optimiser, two different algorithms have been exploited to evaluate which is more appropriate. To further refine the methods, the effects of location, length and height of the surface feature are assessed.

II. Methodology

The optimisation of an aerofoil profile has been examined using both gradient-based and genetic algorithm techniques, with the aim of prolonging the region of laminar flow of the boundary layer. The effect of the inclusion of a surface depression upstream of the neutral stability point on the aerofoil optimisation is assessed, including the influence of the level of detail the aerofoil geometry passed to the optimisation function. Within the framework, Kulfan's class function/shape function transformations (Kulfan, 2008) have been employed for the geometric definition, with the stability calculations based on a linear non-parallel solution. A preliminary study also presents an examination of how the characteristics of the depression are significant with respect to the transitional characteristics of the boundary layer, feeding into future optimisation studies.

A. Optimisation

The purpose of the optimisation is to generate a profile for an infinite swept wing with extension of the laminar region relative to a NACA0012 baseline case. To facilitate this, two optimisation algorithms have been utilized; gradient-based and genetic algorithms, to compare the performance of both schemes for the optimisation of an aerofoil profile in the presence of a small surface deviation. Gradient-based schemes tend to be fast but are liable to get stuck in local minima as they require the computation of derivatives. Investigations using gradient-based optimisation have shown that it is possible for the algorithm to be sensitive to the initial starting point (Montastruc, 2004) and thus resulting in a solution that is not the global optimum. However, they do offer a rapid method of finding local optima and are often much less computationally expensive when compared to genetic algorithms. The genetic algorithm is a global stochastic search technique inspired from evolutionary biology. It operates by randomly generating a 'population' of solutions, with each population evaluated to determine its fitness to the objective function. This fitness is used to create a new population by three operations; reproduction, crossover and then mutation. This process is looped until an optimum solution is found. If the response surface is noisy, consisting of many local minima, a genetic algorithm offers a better chance of obtaining the optimal solution (Vicini, 1998). The chief limitation of genetic algorithms originates in their comparatively poor computational efficiency; an extremely large set of evaluations of the objective function are generally required in order to generate an optimal solution. This becomes of upmost concern when each evaluation is expensive (time/computational resources), and can render genetic algorithms impractical in many instances.

The framework for the optimisation is summarized in Figure 1. The geometry of the aerofoil is created and passed to the infinite swept wing boundary layer program. Stability calculations are performed on the boundary layer profile and an estimate for transition position acquired. The optimisation algorithm then alters the aerofoil profile with the aim of delaying transition as far downstream as possible. This process repeats until an optimal solution is obtained.

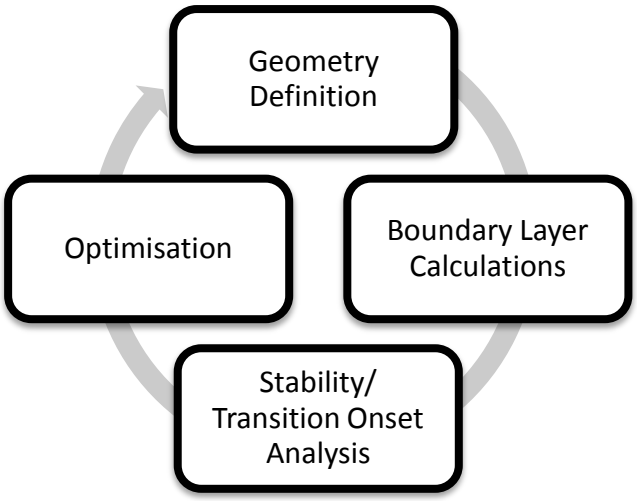

Figure 1. Optimisation procedure

The objective of the aerofoil shape optimisation is solely to delay transition, so no structural functions have been included as bounding conditions. The optimisation problem is formulated from the weighting coefficients that scale the component shape functions in Kulfan's class function/shape function transformations used in the geometry definition. Kulfan's transformations permit aerofoil profiles to be stored in a few variables, which is particularly valuable for optimisation problems. To generate realistic aerofoil shapes, Kulfan's methodology uses Bernstein polynomials to store elements of the geometric data. Two separate optimisation cases with different orders of Bernstein polynomial to represent the surfaces of the aerofoil are presented. Bernstein polynomials of order 3 and 6 were chosen, thus creating the two separate sets, one with 4 design variables and the other with 7.

The upper and lower bounds for the optimisation are provided by approximations of NACA0012 and NACA747a315, arbitrarily chosen for the abundance of geometric data sources available. To obtain the weighting coefficients for the bounds, Kulfan class function/shape function transformations were matched to the known aerofoil profile (NACA0012 or NACA747a315), using a gradient-based optimisation function to perform the fitting and acquire the coefficient values. These bounds were then rounded allowing NACA0012 or NACA747a315 to be encompassed within the extremities. Customization of the bounds can be performed for specific design problems, though with the study being an evaluation of a method the selected constraints were deemed appropriate.

Table 1. Weighting coefficient bounds for order 3 upper surface and lower surface

Upper Surface	TCu_1	TCu_2	TCu_3	TCu_4
Upper Bounds	0.20	0.30	0.30	0.16
Lower Bounds	0.16	0.14	0.14	0.07
Lower Surface	TCl_1	TCl_2	TCl_3	TCl_4
Upper Bounds	-0.11	-0.09	-0.23	-0.11
Lower Bounds	-0.17	-0.16	-0.22	-0.16

Table 2. Weighting coefficient bounds for order 6 upper surface and lower surface

Upper Surface	SCu_1	SCu_2	SCu_3	SCu_4	SCu_5	SCu_6	SCu_7
Upper Bounds	0.16	0.15	0.17	0.11	0.14	0.11	0.04
Lower Bounds	0.21	0.24	0.28	0.33	0.18	0.28	0.19
Lower Surface	SCl_1	SCl_2	SCl_3	SCl_4	SCl_5	SCl_6	SCl_7
Upper Bounds	-0.12	-0.08	-0.16	-0.07	-0.17	-0.10	-0.02
Lower Bounds	-0.18	-0.16	-0.28	-0.12	-0.20	-0.24	-0.19

Figure 2 shows the bounds for the optimisation problem, the larger group formed from the positively defined x surface upper bounds and the negatively defined x surface lower bounds, and vice versa for the smaller group. The slight differences in the bounds for the Order 3 and Order 6 arise due to the approximation of the NACA0012 and NACA747a315 for the different degree of Bernstein polynomial.

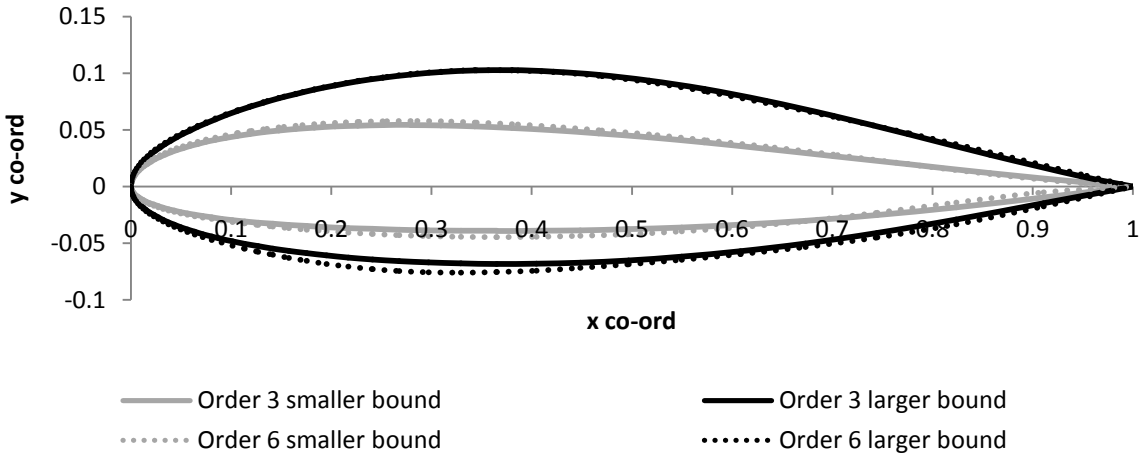

Figure 2. Shape of aerofoil bounds

The gradient-based optimisation was developed using MATLAB, and is initialised with an estimate. From there it attempts to find a constrained minimum of a function of several variables. Within the framework demonstrated in Figure 1, the optimisation problem for order 3 and 6 geometries on the upper and lower surfaces of the aerofoil was solved using the predefined active-set algorithm (*fmincon*). For both upper surface sets (orders 3 and 6), cases were run clean (without depression) and with the inclusion of the depression at a fixed geometric location to first assess the effects of a necessary surface protrusion on the optimal profile. For comparison, a genetic algorithm was implemented within the same framework and the order 3 upper surface cases (with and without a depression) evaluated for comparison with the gradient-based optimised solutions.

The stability calculations are initialized using the reference profile of the NACA0012 for the eigenvalues and starting station. If this fails to find a solution for the new aerofoil geometry, an iterative approach is adopted in order to identify the appropriate eigenvalue/starting station combination. Once a suitable combination has been found, the continuation method is turned on and the starting station is moved as far upstream as possible. Once the stability calculations have been completed, an interpolation method is used to approximate where transition occurs for N = 5 (this value was chosen for ease of future experimental validation within resources available at Queen's University). The purpose of the investigation at this point is to evaluate the developed method, rather than to produce a working aerofoil profile.

B. Geometry Definition

For aerodynamic optimisation, minimizing the required number of design variables is favourable due to the reduction in computational expense. This is especially beneficial for including small surface deviations, as it eliminates the need of redefining all the geometric data at each step. To facilitate this, Kulfan's class function/shape function transformations (Kulfan, 2008) have been employed. Kulfan introduced a class function that defines fundamental classes of aerofoils and axisymmetric bodies with the shape function which define unique geometric shapes within each of these classes. A full description of the implementation is given in Kulfan (2008) but an overview is given here. An aerofoil's geometric coordinates can be described by defining a shape function and identifying its geometry class:

$$\zeta(\psi) = C_{N2}^{N1}(\psi)S(\psi) + \psi\zeta_T \tag{1}$$

The class function and shape function are represented by:

$$C_{N2}^{N1}(\psi) = (\psi)^{N1}[1-\psi]^{N2} \tag{2}$$

$$S(\psi) \equiv \frac{\zeta(\psi) - \psi\zeta_T}{\sqrt{\psi}[1-\psi]} = \sum_{i=0}^{N} A_i \psi^i \tag{3}$$

For a round nose aerofoil N1=0.5 and N2 =1.0. In order to accommodate cambered aerofoils, separate shape functions are utilized for the upper and lower surfaces. The unit shape function, defined by $S(\psi) = 1$, can be deconstructed into two component shape functions:

$S1(\psi) = 1 - \psi$ refers to a round nose aerofoil with a zero boat-tail angle.
$S2(\psi) = \psi$ refers to an aerofoil with zero nose radius and a finite boat-tail angle.

To generate practical aerofoil shapes, the unit shape function is decomposed using a Bernstein polynomial. For any given order *n*, the Bernstein polynomial is compiled of *n* + 1 terms of the structure such that:

$$S_{r,n}(x) = K_{r,n} x^r (1-x)^{n-r} \tag{4}$$

where *r* =0–*n* and $K_{r,n}$ are the binomial coefficients for the particular component shape function defined as:

$$K_{r,n} \equiv \binom{n}{r} \equiv \frac{n!}{r!\,(n-r!)} \tag{5}$$

To obtain the upper or lower surface coordinates of an aerofoil, component shape functions are used. These component shape functions are scaled by "weighting" coefficients as shown in the subsequent equations. Component shape function:

$$S_i(\psi) = K_i \psi^i (1-\psi)^{n-1} \tag{6}$$

The binomial coefficient K_i, is defined as:

$$K_i \equiv \binom{n}{i} \equiv \frac{n!}{i!\,(n-i!)} \tag{7}$$

Resulting in the overall shape function as:

$$S(\psi) = \sum_{i=1}^{n} A_i\, S_i(\psi) \tag{8}$$

The current work is based on two different orders of the Bernstein polynomial, 3 and 6, as suggested in Kulfan (2008). By changing the weighting coefficients, the profile of the aerofoil is altered, thus giving the design variables for the optimisation problem. The objective function is formulated to discover a combination of weighting coefficients that will give a profile with the greatest extended laminar region.

A small depression, modelled as a cosine bell function, is then superimposed onto the resulting aerofoil profile, with the specified length and height normal to the surface. A baseline of a sweep of 20° for the infinite swept wings, which is known to be a Tollmien-Schlichting dominated flow type, has been selected. The wing is modelled by generating the aerofoil *x* and *y* coordinates (using the method above) in addition to specifying the spanwise stations.

B. Boundary Layer Stability

Calculation of the boundary layer profile over a given surface is performed using a simplified version of the Navier-Stokes equations. For infinite swept wings, the basic flow is independent of the spanwise direction therefore allowing quasi-three dimensional boundary-layer equations to be used to obtain the mean flow. The boundary conditions are obtained from a panel method. The widely used Linear Stability Theory (LST) eigenvalue-based predictions tend to be highly conservative, with a great deal of uncertainty when surface features are included. However, many of these limitations can be overcome through the solution of the partial differential equations with a parabolizing approximation (PSE method). Since the equations have been parabolized, boundary conditions and an upstream boundary condition, sometimes referred to as an initial condition, are needed. For initial upstream conditions most investigations use approximations such as parallel Orr–Sommerfeld theory, or a local solution to the

PSE for initial upstream conditions. For the current work, the initial conditions for the PSE have been obtained by solving linear stability equations. Following the derivation of the PSE for three-dimensional flows (Cebeci, 2004), after ignoring second order terms and subtracting the mean flow equations from the x, y and z momentum equations for incompressible flows, given that;

$$u = \bar{u} + u', v = \bar{v} + v', w = \bar{w} + w', p = \bar{p} + p' \tag{9}$$

The normalized forms of the fluctuating quantities can be written (bars over mean quantities omitted):

$$\frac{\partial u'}{\partial t} + u\frac{\partial u'}{\partial x} + u'\frac{\partial u}{\partial x} + v\frac{\partial u'}{\partial y} + v'\frac{\partial u}{\partial y} + w\frac{\partial u'}{\partial z} + w'\frac{\partial u}{\partial z} = -\frac{1}{\varrho}\frac{\partial p'}{\partial x} + \mathbb{v}\nabla^2 u' \tag{10}$$

$$\frac{\partial v'}{\partial t} + u\frac{\partial v'}{\partial x} + u'\frac{\partial v}{\partial x} + v\frac{\partial v'}{\partial y} + v'\frac{\partial v}{\partial y} + w\frac{\partial v'}{\partial z} + w'\frac{\partial v}{\partial z} = -\frac{1}{\varrho}\frac{\partial p'}{\partial y} + \mathbb{v}\nabla^2 v' \tag{11}$$

$$\frac{\partial w'}{\partial t} + u\frac{\partial w'}{\partial x} + u'\frac{\partial w}{\partial x} + v\frac{\partial w'}{\partial y} + v'\frac{\partial w}{\partial y} + w\frac{\partial w'}{\partial z} + w'\frac{\partial w}{\partial z} = -\frac{1}{\varrho}\frac{\partial p'}{\partial z} + \mathbb{v}\nabla^2 w' \tag{12}$$

With no mean flow variation in the z-direction, the three-dimensional disturbance of q' can be described by:

$$q_j'(x,z,y,t) = q_j(x,y)exp\left\{i\left[\int_{x_0}^{x}\alpha(x)dx + \beta z - \omega t\right]\right\} = q_j e^m \tag{13}$$

where:

$$q_j' = \begin{pmatrix} u' \\ v' \\ w' \\ p' \end{pmatrix} = \begin{pmatrix} f' \\ \phi' \\ g' \\ \Pi' \end{pmatrix} e^m \tag{14}$$

Substituting the differentials of the disturbance functions q_j' into the linearized perturbation equations, reducing q_{xx} to zero (due to the negligible contribution) and using the continuity equation for perturbation quantities:

$$\frac{\partial u'}{\partial x} + \frac{\partial v'}{\partial y} + \frac{\partial w'}{\partial z} = 0 \tag{15}$$

The linear PSE for three-dimensional incompressible flows are obtained as follows:

$$i\alpha f + \phi' + i\beta g = -\frac{\partial f}{\partial x} \tag{16}$$

$$i\xi_1 f + u'\phi + i\alpha\Pi + \frac{1}{R}(\xi_2^2 f - f'') = -\frac{\partial u}{\partial x}f - vf' - u\frac{\partial f}{\partial x} - \frac{\partial \Pi}{\partial x} + \frac{2i\alpha}{R}\frac{\partial f}{\partial x} + \frac{i}{R}\frac{d\alpha}{dx}f \tag{17}$$

$$i\xi_1\phi + \Pi' + \frac{1}{R}(\xi_2^2\phi - \phi'') = -\frac{\partial v}{\partial x}f - v\phi' - v'\phi - u\frac{\partial \phi}{\partial x} - \frac{2i\alpha}{R}\frac{\partial \phi}{\partial x} + \frac{i}{R}\frac{d\alpha}{dx}\phi \tag{18}$$

$$i\xi_1 g + w'\phi + i\beta\Pi + \frac{1}{R}(\xi_2^2 g - g'') = -\frac{\partial w}{\partial x}f - vg' - u\frac{\partial g}{\partial x} + \frac{2i\alpha}{R}\frac{\partial g}{\partial x} + \frac{i}{R}\frac{d\alpha}{dx}g \tag{19}$$

where:

$$\xi_1 = \alpha u + \beta w - \omega, \xi_2^2 = \alpha^2 + \beta^2 \tag{20}$$

Boundary conditions:

$$q_j(x,0) = 0, \;\; q_j(x,\infty) = 0 \tag{21}$$

The above methods allow the transition onset for an aerofoil defined in a small number of variables to be estimated. By formulating an objective function so that the optimisation algorithm can prolong the distance until this transition onset the effectiveness of gradient-based and genetic algorithm techniques can be evaluated, along with screening of depression feature variables that could influence the optimal profile.

III. Results

A. Optimisation Results

Combining the geometric representation and transition methods, as shown in Figure 1, a framework is set up to assist in finding an infinite swept wing aerofoil profile with a prolonged laminar region by varying the weighting coefficients. This section illustrates the combinations of the weighting coefficients produced by using the different optimisation algorithms; (1) gradient-based and (2) genetic algorithm. Transition position is given as percentage chord. All calculations were performed at a Reynolds numbers of 5 million and at 0° angle of attack.

(1) Gradient-based optimisation

The results of the following are presented; Bernstein polynomial of orders 3 and 6, with/without depression and different starting profiles for the optimisation. If the depression is to be included, its characteristics are length 4%$\overline{c}$, height 0.0005% $\bar{c}$, located at 8%$\overline{c}$. The different starting profiles were chosen to assist in the assessment of whether the optimisation algorithm was getting stuck in local minima, and were selected to be close to opposite extremities of the bounds.

Upper Surface

Table 3. Order 3 without depression

Case	Approximate Starting Profile	TCu_1	TCu_2	TCu_3	TCu_4	Transition Onset
(a)	NACA0012	0.160	0.211	0.147	0.08	36.9%
(b)	NACA747a315	0.190	0.292	0.299	0.07	46.9%

Table 4. Order 3 with depression

Case	Approximate Starting Profile	TCu_1	TCu_2	TCu_3	TCu_4	Transition Onset
(c)	NACA0012	0.175	0.140	0.300	0.160	50.0%
(d)	NACA747a315	0.195	0.291	0.299	0.07	47.5%

Table 5. Order 6 without depression

Case	Approximate Starting Profile	SCu_1	SCu_2	SCu_3	SCu_4	SCu_5	SCu_6	SCu_7	Transition Onset
(e)	NACA0012	0.160	0.150	0.170	0.325	0.140	0.280	0.04	55.2%
(f)	NACA747a315	0.197	0.205	0.192	0.330	0.180	0.280	0.09	54.9%

Table 6. Order 6 with depression

Case	Approximate Starting Profile	SCu_1	SCu_2	SCu_3	SCu_4	SCu_5	SCu_6	SCu_7	Transition Onset
(g)	NACA0012	0.178	0.150	0.170	0.327	0.142	0.257	0.05	57.0%
(h)	NACA747a315	0.182	0.194	0.170	0.323	0.179	0.250	0.04	52.5%

Lower Surface

Table 7. Order 3

Approximate Starting Profile	TCl_1	TCl_2	TCl_3	TCl_4	Transition Onset
NACA0012	-0.169	-0.138	-0.133	-0.143	23.3%

Table 8. Order 6

Approximate Starting Profile	SCl_1	SCl_2	SCl_3	SCl_4	SCl_5	SCl_6	SCl_7	Transition Onset
NACA0012	-0.129	-0.133	-0.181	-0.119	-0.17	-0.100	-0.19	25.0%

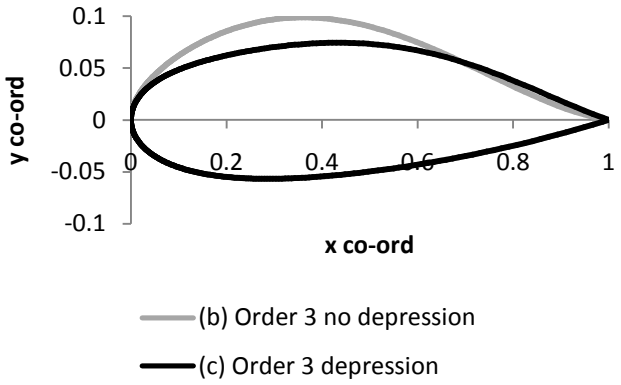

Figure 3. Optimal Order 3 depression/no depression comparison

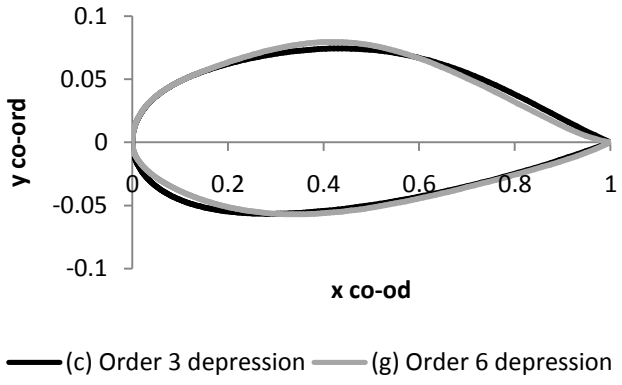

Figure 4. Optimal Order 3 depression/Order 6 depression

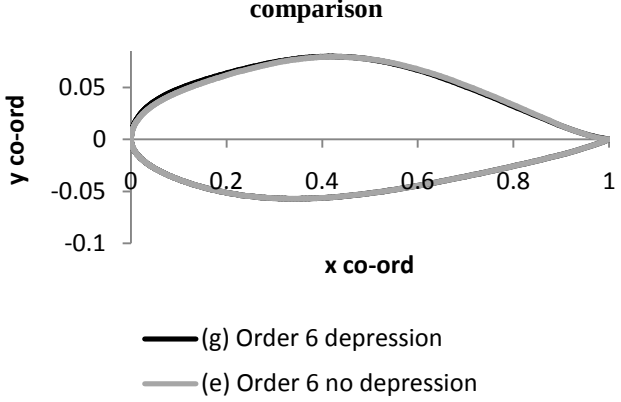

Figure 5. Optimal Order 6 depression/no depression comparison

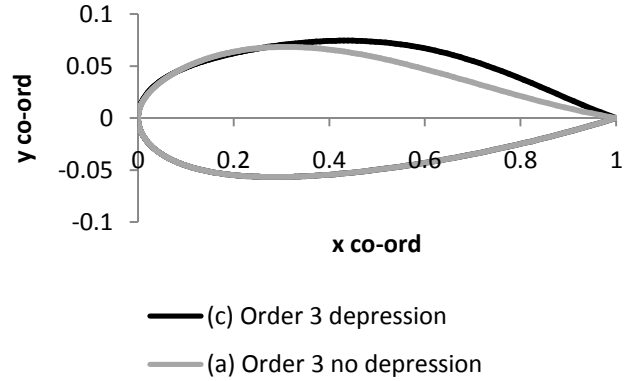

Figure 6. Order 3 depression/no depression comparison NACA0012 starting profile

(2) Genetic algorithm optimisation

Undertaking the optimisation with a genetic algorithm, the calculations on the upper surface of an aerofoil of Bernstein polynomial order 3 with/without depression (located at x = 8%, length = 4%, height = 0.0005% if included) are presented. No starting profiles are required when using a genetic algorithm and the boundary conditions are kept the same as the gradient-based technique for comparison.

Upper Surface

Table 9. Order 3 with depression

Case	TCu_1	TCu_2	TCu_3	TCu_4	Transition Position
(i)	0.164	0.175	0.296	0.152	58.6%

Table 10. Order 3 without depression

Case	TCu_1	TCu_2	TCu_3	TCu_4	Transition Position
(j)	0.163	0.180	0.300	0.140	57.8%

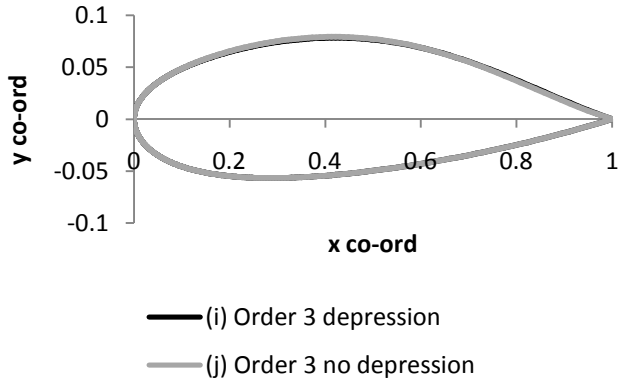

Figure 7. Optimal GA Order 3 depression/no depression comparison

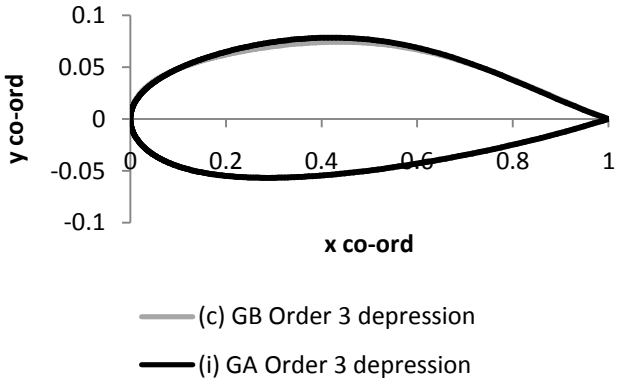

Figure 8. Optimal GB Order 3 depression/GA depression comparison

From the results presented above it is clear that the optimisation process using a gradient-based method is sensitive to the initial point used to start the optimisation, the exclusion/inclusion of a depression and order of Bernstein polynomial. When using a genetic algorithm the transition onset is delayed considerably relative to both the baseline profile and the optimal profile obtained from the gradient-based method, and the aerofoil profiles have converged on a similar solution independent of depression inclusion which is not always the case observed with the gradient-based technique.

B. Depression

The results from the previous section demonstrate that the inclusion of a surface feature has an influence on the optimisation process. The sensitivity can be quite dramatic, as shown in Figure 6, or rather less pronounced as seen in Figures 5 and 7. It appears that the inclusion of the depression on the aerofoil surface can alter the search path of the optimisation algorithm and has an effect on the response surface obtained, but the nature of this modified response surface is not entirely clear. This section will look in more detail at how the surface feature itself affects the results of the PSE, thus performing a screening of variables and comment on the implication of this for the optimisation.

If investigating for the optimal combination of aerofoil profile and surface deviation it is necessary to have identified what depression variables are significant. Presented are results on the location, length and height of the depression with the sole aim of identifying if they have an appreciable effect on the stability characteristics. An example shown in figure 9 compares a default NACA0012 profile with an aerofoil geometry including a depression of length 4%$\overline{c}$, height 0.0005% $\bar{c}$, located at 8%$\overline{c}$.

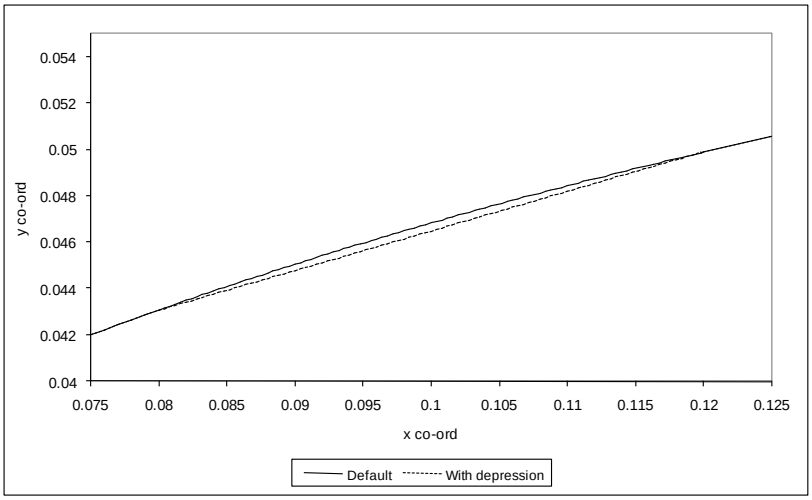

Figure 9. Section of NACA0012 profile with/without depression

While retaining the baseline NACA0012 profile, it is assessed whether the characterizing features (length, height, streamwise location) of the depression will have an effect on the results outputted by the PSE. This permits conclusions on whether each of these surface feature variables are required to be considered in optimisation processes intending to enhance roughness element design. Figure 10 shows a comparison of the frequency amplification with (k) the depression located at an optimal location ahead of the neutral stability point (l) the depression located behind the neutral stability point. Locating the depression at (l) has the effect of promoting the transition to turbulence to an earlier stage.

All calculations were performed at a Reynolds numbers of 5 million and at 0° angle of attack.

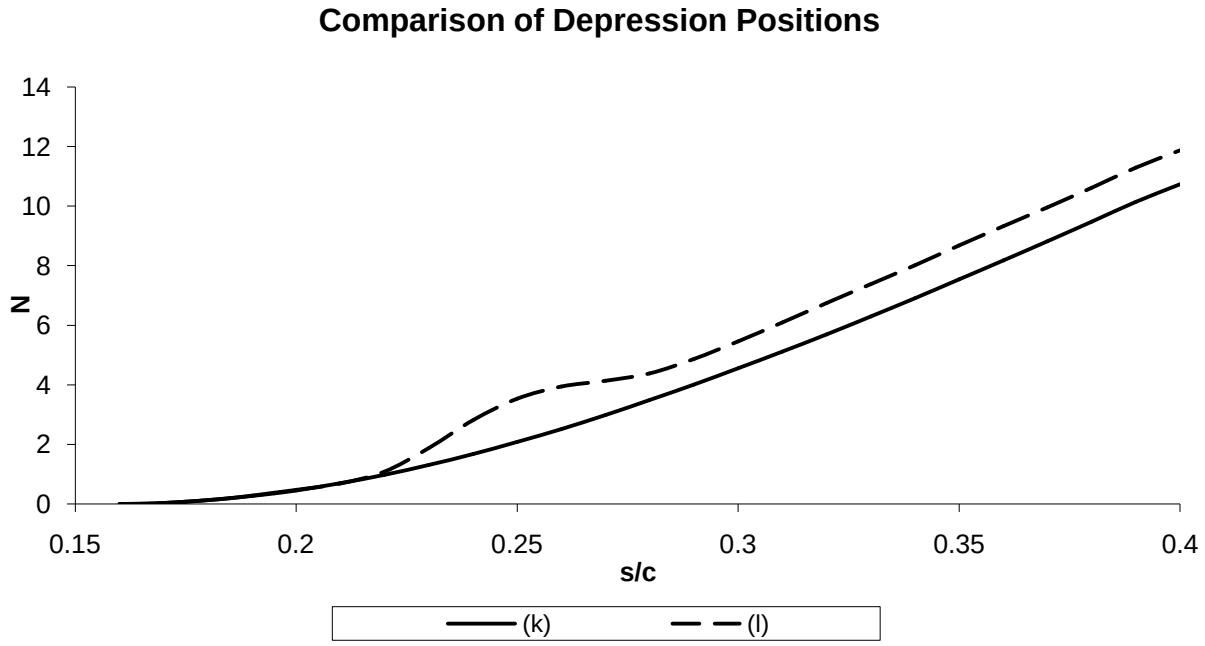

Figure 10. NACA0012 profiles with/without leading edge depression
(k) Depression located at x = 8%, length = 4%, height = 0.0005%
(l) Depression located at x = 20%, length = 4%, height = 0.0005%

Figure 11 demonstrates the effect of changing the height by a factor of 10 while keeping the length at 4%$\bar{c}$ (located at 20%$\bar{c}$). Figure 12 shows results of altering the length from 2% to 4%, with the same height (depression situated at 8%$\bar{c}$).

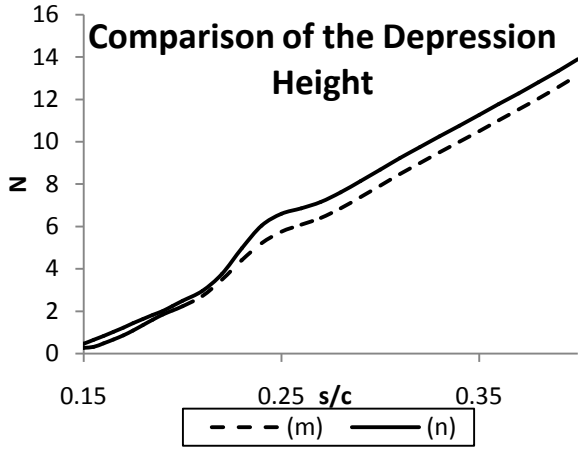

Figure 11. Influence of height

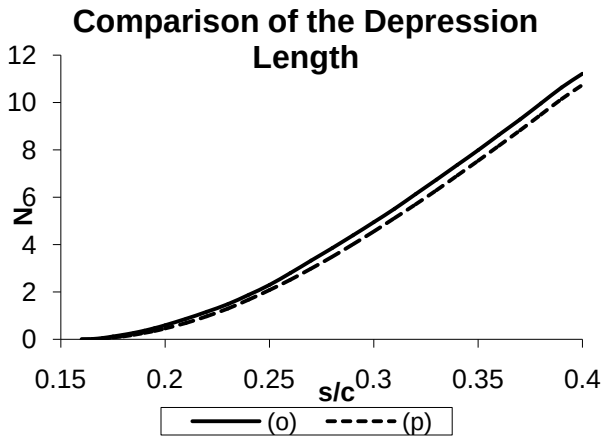

Figure 12. Influence of length

(m) Depression located at x = 20%, length = 4%, height = 0.0005%

(n) Depression located at x = 20%, length = 4%, height = 0.005%

(o) Depression located at x = 8%, length = 2%, height = 0.0005%

(p) Depression located at x = 8%, length = 4%, height = 0.0005%

As an appreciable difference is demonstrated in each Figure (10 -12) the surface feature location, height and length all need to be investigated if they were to be included in the optimisation framework.

IV. Discussion

The results of the gradient-based optimisation indicate that the response surface has many local minima, and the final profile generated is heavily dependent on the starting values used, the order of the Bernstein polynomial and whether a depression is included or not. As shown in Tables 3-6, the starting point for the optimisation process has significant impact on the result, the most prominent difference arising in the order 3 with no depression case. Figure 3 shows (when compared to Figure 4 etc.) that this case has produced a result that is considerably different than the best possible profiles from all the others, suggesting that a range of starting profiles is critical to ensuring a sensible result is achieved, and that even minor modifications can lead to significantly different outputs. Order 6 Bernstein polynomials do not offer any notable advantage when using this framework, and enlarge the computational expensive considerably (by approximately a (minimum) factor of 4, thus negating the main advantage of using gradient-based algorithms). However, the Order 6 polynomial does appear to be less sensitive to the noisy response surface (as noted in Figure 5/Tables 5 and 6), with less variation in the converged solutions obtained.

The addition of the depression in the surface alters the optimal profile obtained, shifting the search path the optimisation algorithm pursues and consequently can result in a dramatically different profile to that obtained for the clean cases. A profile has been identified which extends the laminar region from 36.9% to 50% for the given conditions, thus shifting the solution from one local minimum to another (Figure 6). It is evident that the framework that uses a gradient-based optimisation algorithm is highly sensitive to the inputs (starting profile, inclusion of depression (or not), order of Bernstein polynomial), and with such significant variation on the final results depending on these inputs indicates that gradient-based techniques are not suited to this type of optimisation problem.

When comparing the bounds between the different orders of Bernstein polynomial, there are minor variations in the profiles the weighting coefficients produce. Difficulty arises when trying to keep the shape of the bounds between different orders of Bernstein polynomial identical. Trying to match the order 6 upper bound with an order 3 polynomial, using the process mentioned in the methodology to find weighting coefficients, resulted in coefficients that were dissimilar to those for a 3rd order Bernstein polynomial for NACA747a315. Therefore the decision to round the upper and lower bounds to encompass the real world profiles was made.

The profiles generated for the upper surface of the aerofoil by the genetic algorithm for the order 3 Bernstein polynomial have converged on a solution which is in stark contrast to the gradient-based technique. The with/without depression aerofoil profiles, as seen in Figure 7, have converged on a very similar solution, unlike those obtained with a gradient-based optimiser (Figure 3). They also offer a considerable improvement on the transition onset location, shifted up to approximately 58% compared to 50% generated by gradient-based methods. Figure 8 demonstrates that the gradient-based method can create comparably shaped optimal profiles, but with the response surface so sensitive, a genetic algorithm is needed to avoid non-optimal local minima and ensure that a approximate optimal solution, rather than a local minima, is being obtained. When dealing with surface features, changes in the transition onset are likely to be of a small magnitude so it is highly critical to have an optimisation algorithm that is robust, suggesting that for this framework, genetic algorithms are better suited.

Although the depression features were fixed during the optimisation (location, height, length), for an investigation looking for the optimal aerofoil profile and surface deviation (for examples, designing joints or rivets) it is essential to know what depression variables are important. From the results in Figures 10, it is clear that the location of the depression appears to have a dramatic effect on the site of the breakdown to turbulence. Figure 11 and Figure 12 demonstrate that altering the depression length and height results in more changes to the stability characteristics. It can be concluded that all these variables, location, height and length would need to be included in the objective function to find the optimal type of depression on the aerofoil.

V. Conclusions

From the studies undertaken, it has been shown that it is possible to create an environment to optimise the profile of an infinite swept wing for extended regions of laminar flow along its profile with the inclusion of small scale roughness elements. When using gradient-based methods, there is an inclination for the algorithm to tend towards local minima, and due to the nature of the response surface, the minima is approaches is highly dependent on the initial conditions defined. Whether a surface feature is included or not, the starting position and order of Bernstein polynomial all have an effect on the path the gradient-based algorithm searches, generating different optimal profiles thus producing inconsistency in the results obtained. By sacrificing the quick runtime of using a gradient-based method, consistent outcomes can be attained by implementing a genetic algorithm. With the inclusion of surface features, the tendency of the gradient-based technique to output a non-optimal solution is highly restrictive with the nature of the stability of flows so sensitive. Therefore it is concluded that a genetic algorithm is more appropriate within this type of optimisation structure. Screening of variables to define the depression feature indicate that shape is a significant factor to consider, particularly if a depression is located close to the point of neutral stability, and for this reason, it is necessary to fully define the height and length of such a depression (with appropriate bounds) in order to fully represent the effects of such a feature on the aerodynamic design optimisation process.

References

Atkin, C. (2008) " Laminar Flow Control: Leap or Creep?" 38th Fluid Dynamics Conference and Exhibit, Seattle, Washington, June 23-26, 2008

Cebeci, T (2004) *Stability and Transition: Theory and Application* 1st ed., Horizons Publishing Inc., Long Beach, 2004

Choi, K.S. & Fujisawa, N. (1993) " Possibility of drag reduction using-type roughness" Applied Scientific Research, Volume 50, Numbers 3-4 / May, 1993

Crouch, (1997) "Transition prediction and control for airplane applications" Fluid Dynamics Conference, 28th, Snowmass Village, CO, June 29-July 2, 1997

Gaster & Wang (2005) "Effect of surface steps on boundary layer transition" Experiments in Fluids (2005), 38 679-686, 2005

Joslin, R (1998) "Aircraft Laminar Flow Control," Annual Review of Fluid Mechanics Vol. 30: 1-29 1998

Kulfan, B (2008) "Universal Parametric Geometry Representation Method," Journal of Aircraft
Vol. 45, No. 1, January–February 2008

Montastruc, L (2004) "Use of genetic algorithms and gradient based optimisation techniques for calcium phosphate precipitation," Laboratoire de Génie Chimique, UMR CNRS/INP/UPS 5503, ENSIACET, 118 Route de Narbonne, 31077, Toulouse Cedex 04, France,3 2004

Reed, H. & Saric, W. (2008) "Transition Mechanisms for Transport Aircraft" 38th Fluid Dynamics Conference and Exhibit, Seattle, Washington, June 23-26, 2008

Reshotko, E. (1994) "Boundary layer instability, transition and control" Aerospace Sciences Meeting and Exhibit, 32nd, Reno, NV, Jan 10-13, 1994

Saric, W. & Reed, H. (2004) "Toward Practical Laminar Flow Control - Remaining Challenges" 2nd AIAA Flow Control Conference, Portland, Oregon, June 28-1, 2004

Saric, Carillo & Reibert (1998) "Leading-Edge Roughness as a Transition Control Mechanism" AIAA paper, 1998

Vicini, A (1998) "Airfoil and Wing Design through Hybrid Optimization Strategies" AIAA paper, 1998